Semi-analytic technique for analyzing mode-locked lasers

Nicholas G. Usechak and Govind P. Agrawal

The Institute of Optics, University of Rochester, Rochester, New York 14627 and Laboratory for Laser Energetics, University of Rochester, Rochester, New York 14623

gpa@optics.rochester.edu

Abstract: A semi-analytic tool is developed for investigating pulse dynamics in mode-locked lasers. It provides a set of rate equations for pulse energy, width, and chirp, whose solutions predict how these pulse parameters evolve from one round trip to the next and how they approach their final steady-state values. An actively mode-locked laser is investigated using this technique and the results are in excellent agreement with numerical simulations and previous analytical studies.

OCIS codes: (140.3430) Lasers, theory; (140.4050) Mode-locked lasers; (140.3510) Lasers, fiber;

References and links

1. D. J. Kuizenga and A. E. Siegman, "FM and AM Mode Locking of the Homogeneous Laser–Part I: Theory," IEEE J. Quantum Electron. **QE-6**, 694-708 (1970).
2. S. N. Vlasov, V. A. Petrishchev, and V. I. Talanov "Averaged description of wave beams in linear and nonlinear media (the method of moments)," Radiophys. Quantum Electron. **14**, 1062-1070 (1971).
3. C. J. McKinstrie, "Effects of filtering on Gordon-Haus timing jitter in dispersion-managed systems," J. Opt. Soc. Am. B **19**, 1275-1285 (2002).
4. J. Santhanam and G. P. Agrawal, "Raman-induced spectral shifts in optical fibers: general theory based on the moment method," Opt. Commun. **222**, 413-420 (2003).
5. H. A. Haus and Y. Silberberg, "Laser Mode Locking with Addition of Nonliner Index," IEEE J. Quantum Electron. **QE-22**, 325-331 (1986).
6. G. P. Agrawal, *Applications of Nonlinear Fiber Optics* (Academic Press, New York, 2001).
7. F. X. Kärtner, D. Kopf, and U. Keller, "Solitary-pulse stabilization and shortening in actively mode-locked lasers," J. Opt. Soc. Am. B **12**, 486-496 (1995).

1. Introduction

Mode-locked lasers are routinely used for a wide variety of applications since they can provide optical pulses ranging in widths from a few femtoseconds to hundreds of picoseconds. As early as 1970, an analytic theory was developed for determining pulse parameters and shape in actively mode-locked solid-state lasers by considering the effects of the mode-locker and gain filtering and then imposing a self-consistency criterion in the time domain [1]. In many cases, it is possible to include the effect of chromatic dispersion on the pulse shape as well; however, once the nonlinear effects within the cavity become important, analytic investigations begin to falter. This is frequently the case in fiber lasers where both fiber dispersion and nonlinearity are important.

In this work, we develop a new tool for investigating mode-locked lasers by essentially treating the mode-locked pulses as particles with a fixed analytic shape. This approach allows us to simplify the governing nonlinear partial differential equation, often called the master equation

#6418 - $15.00 US Received 26 January 2005; revised 9 March 2005; accepted 9 March 2005

of mode-locking, into a set of coupled ordinary differential equations. The resulting equations are similar to the rate equations commonly used to describe continuously operating lasers. They can be solved quickly using standard techniques and have the added benefit that under steady-state conditions they reduce to algebraic equations describing pulse energy, width, and chirp. These algebraic equations indicate the trade-offs associated with the different laser parameters and overcome any issues associated with computation time. Our approach represents an application of the moment method [2], a technique used extensively within the field of telecommunications [3, 4], to the case of a mode-locked laser.

Aside from experimental measurements, full numerical simulations provide the best means to determine the exact shape of a mode-locked pulse. However, numerical studies tend to be time consuming, making extensive exploration of the parameter space difficult. This issue is particularly acute in fiber lasers, where thousands of round trips are necessary before a stable solution emerges. Although mode-locked pulses require characterization when used for experimental purposes, the pulse parameters are usually more important than the exact pulse shape. Moreover, pulse shape is invariably close to Gaussian or hyperbolic secant, depending on the type of mode-locking employed, the cavity dispersion (normal vs. anomalous), and the strength of nonlinearities. This observation is at the root of our approach since the moment method requires a knowledge of the pulse shape. Despite this apparent limitation, one is able to retain a high degree of accuracy in the pulse parameters if a judicious choice is made for the pulse shape.

2. The master equation of mode-locking

If the dispersive and nonlinear effects are relatively weak over a single round trip, the temporal shape and width of the pulse change little during this period (assuming the mode-locker's effect on the field is weak and discrete losses are minimal). Although an approximate treatment, it is fair to model such a system by the master equation of mode-locking [5] obtained by averaging over the round-trip cavity length L_R. This equation takes the form [5, 6]

$$T_R\frac{\partial A}{\partial T}+\frac{i}{2}\left(\bar{\beta}_2+i\bar{g}T_2^2\right)L_R\frac{\partial^2 A}{\partial t^2}=i\bar{\gamma}L_R|A|^2A+\frac{1}{2}\left(\bar{g}-\bar{\alpha}\right)L_RA+M(A,t), \tag{1}$$

where $T=z/v_g$, v_g is the group velocity, and $A(T,t)$ is the slowly varying envelope of the electric field. As in Refs. [5, 7], we have assumed second-order dispersion dominates; therefore higher-order dispersive effects have been ignored in Eq. (1). It is important to note there are two time scales in this equation; the time t measured in the frame of the moving pulse and the propagation time T, often called the coarse-grained time [7]. Since we averaged over a single round trip, T is measured in terms of the round-trip time $T_R=L_R/v_g$. It is assumed that the time scale associated with the pulse is sufficiently smaller than T_R so the two times are essentially decoupled. This treatment is valid for most lasers for which T_R exceeds 1 ns and pulse widths are typically less than 100 ps.

In rare-earth-doped fibers, the gain medium responds on a time scale much slower than the round-trip time, and the saturated gain may be approximated by $\bar{g}=\bar{g}_0\left(1+P_{\text{ave}}/P_{\text{sat}}\right)^{-1}$ where P_{ave} represents the average power defined as

$$P_{\text{ave}}=\frac{1}{T_m}\int_{-T_m/2}^{T_m/2}|A(t,z)|^2\,dt. \tag{2}$$

The same treatment is valid for many non-fiber lasers as well [5]. In Eq. (2) $T_m=F_{\text{rep}}^{-1}=m^{-1}T_R$, where m is an integer representing the harmonic the laser is mode-locked at and F_{rep} is the repetition rate of the pulses. The overbar in Eq. (1) denotes the value of the corresponding parameter

#6418 - $15.00 US Received 26 January 2005; revised 9 March 2005; accepted 9 March 2005

averaged over a round trip. More specifically, $\bar{\beta}_2$ represents the averaged second-order dispersion of the cavity elements, while $\bar{\gamma}$ takes into account the averaged nonlinear parameter and $\bar{\alpha}$ represents the averaged losses. The finite gain bandwidth is assumed to have a parabolic filtering effect with a spectral full width at half maximum (FWHM) given by $\Delta_w = 2/T_2$.

In the absence of the mode-locker, Eq. (1) reduces to the well-known Ginzberg–Landau equation, which supports a shape-preserving solution in the anomalous-dispersion regime known as the autosoliton and given by [6]

$$A(T,t) = a\left[\operatorname{sech}(t/\tau)\right]^{1+iq} \exp\left[i\phi\left(T\right)\right], \tag{3}$$

where the pulse parameters a, τ, q, and $\phi(T)$ are determined uniquely by the parameters appearing in Eq. (1). In the absence of a mode-locker, a stable pulse will neither form nor survive multiple round trips in the cavity. However, the active fiber will try to impose the autosoliton shape on any pulse circulating in such a laser. This fact was previously exploited by Haus and Silberberg in their investigation of pulse shortening in AM mode-locked lasers in the presence of dispersive and nonlinear elements [5]. In this work we assume that the laser is mode-locked with the autosoliton shape; we then seek to include the effects of the mode-locker on the pulse energy, width, and chirp. To extend our analysis to the normal-dispersion regime, we also consider a chirped Gaussian pulse

$$A(T,t) = a\left[\exp\left(-t^2/2\tau^2\right)\right]^{1+iq} \exp\left[i\phi\left(T\right)\right]. \tag{4}$$

3. The moment method

In an effort to study the pulse evolution process under the influence of Eq. (1), without resorting to full numerical simulations, we have employed the moment method [2–4]. This approach allows us to develop ordinary differential equations that govern the evolution of the pulse parameters. These equations can be solved quickly, yielding the information of experimental interest. All of this, however, is based on a knowledge of the exact pulse shape. For this reason, one should also solve Eq. (1) to ensure that the actual pulse shape does not deviate much from the assumed pulse shape. Experimentally, the results obtained from autocorrelation measurements, electric-field reconstruction, or an optical spectrum analyzer may be used to validate a particular ansatz.

As seen in Eqs. (3) and (4), a mode-locked pulse is characterized by four parameters, amplitude a, width τ, chirp q, and phase $\phi(T)$. The phase is rarely of physical interest in lasers producing picosecond pulses, and we ignore it in the following discussion for brevity. The amplitude can easily be related to energy and so we focus on pulse energy E, width τ, and chirp q. These parameters can be defined as moments of $A(T,t)$ [4]:

$$E(T) = \int_{-\infty}^{\infty} |A(T,t)|^2 \, dt, \tag{5}$$

$$\tau^2(T) = \frac{2}{C_1 E} \int_{-\infty}^{\infty} t^2 \, |A(T,t)|^2 \, dt, \tag{6}$$

$$q(T) = \frac{i}{E} \int_{-\infty}^{\infty} t \left[A^* \frac{\partial A}{\partial t} - A \frac{\partial A^*}{\partial t} \right] dt, \tag{7}$$

where the constant C_1, defined in the next section, converts the root-mean-square width into pulse width τ. To investigate how our pulse parameters evolve during propagation, we differentiate Eqs. (5)–(7) with respect to T yielding

$$\frac{dE}{dT} = \int_{-\infty}^{\infty} \left[A^* \frac{\partial A}{\partial T} + A \frac{\partial A^*}{\partial T} \right] dt, \tag{8}$$

#6418 - $15.00 US Received 26 January 2005; revised 9 March 2005; accepted 9 March 2005

$$\tau\frac{d\tau}{dT} = -\frac{1}{2E}\frac{dE}{dT}\tau^2 + \frac{1}{C_1 E}\int_{-\infty}^{\infty} t^2\left[A^*\frac{\partial A}{\partial T} + A\frac{\partial A^*}{\partial T}\right]dt, \tag{9}$$

$$\frac{dq}{dT} = -\frac{1}{E}\frac{dE}{dT}q + \frac{i}{E}\int_{-\infty}^{\infty} t\left[\frac{\partial}{\partial T}\left(A^*\frac{\partial A}{\partial t}\right) - \frac{\partial}{\partial T}\left(A\frac{\partial A^*}{\partial t}\right)\right]dt. \tag{10}$$

The final step consists of substituting $\partial A/\partial T$ from Eq. (1) into Eqs. (8)–(10), picking a pulse shape such as those given in Eq. (3) or (4), and integrating over t using a specific mode-locking mechanism.

4. Mode-locking rate equations

To continue, we need to specify the mechanism used to mode-lock the laser. Mode-locking via amplitude modulation (AM) is one of the oldest techniques; we focus on it to illustrate our approach by using $M(A,t) = -\Delta_{AM}[1-\cos(\omega_m t)]A$ in Eq. (1), where Δ_{AM} is the modulation depth experienced by a pulse during a single round trip, $\omega_m = 2\pi/T_m$ is the modulation frequency (assumed to be identical to the repetition rate of the mode-locked pulse train), and the average loss of modulator has been incorporated into $\bar{\alpha}$. Assuming that the mode-locked pulses are much shorter than T_m, we approximate the effect of the AM mode-locker as $M(A,t) \approx -\Delta_{AM}\omega_m^2 t^2/2A$. Although this approximation is not required, it simplifies the appearance of the equations in the rest of this paper and is applicable in most cases of practical interest.

Using Eqs. (3) and (4) for the pulse shape, and performing the integration in Eqs. (8)–(10) we obtain the following equations:

$$\frac{T_R}{E}\frac{dE}{dT} = (\bar{g}-\bar{\alpha})L_R - C_0\frac{\bar{g}T_2^2 L_R}{2\tau^2}\left(1+q^2\right) - \frac{1}{2}C_1\Delta_{AM}\omega_m^2\tau^2, \tag{11}$$

$$2\tau T_R\frac{d\tau}{dT} = \left(2\bar{\beta}_2 L_R/C_1\right)q + C_2\bar{g}T_2^2 L_R\left(C_3-q^2\right) - C_4\Delta_{AM}\omega_m^2\tau^4, \tag{12}$$

$$\tau^2 T_R\frac{dq}{dT} = C_0\bar{\beta}_2 L_R\left(1+q^2\right) - C_5\bar{g}T_2^2 L_R\left(1+q^2\right)q + C_6\frac{\bar{\gamma}L_R E\tau}{\sqrt{2\pi}} - C_1\Delta_{AM}\omega_m^2\tau^4 q, \tag{13}$$

where the constants C_n ($n = 0$ to 6) are introduced such that they all equal 1 for a Gaussian pulse. In the case of an autosoliton, $C_0 = 2/3$, $C_1 = \pi^2/6$, $C_2 = 4/\pi^2$, $C_3 = 2$, $C_4 = 4\pi^2/15$, $C_5 = 1/3$, and $C_6 = \sqrt{2\pi}/3$.

Equations (11)–(13) are analogous to the rate equations used for continuous-wave lasers in the sense that they describe how the pulse parameters E, τ, and q change from one round trip to the next. For example, Eq. (11) shows that the energy is enhanced by the gain (first term) but reduced by both the gain filtering (second term) and the AM mode-locker (third term). Similarly, Eq. (12) shows that the modulator shortens optical pulses as they pass through it (last term).

To illustrate pulse dynamics, we solve Eqs. (11)–(13) for a fiber-ring laser using realistic parameter values. More specifically, we use $\beta_2 = \pm 0.014$ ps^2/m, $\bar{\gamma} = 0.012$ W^{-1}/m, $\bar{g}_0 = 0.55$ m^{-1}, $\bar{\alpha} = 0.17$ m^{-1}, $T_2 = 47$ fs/rad, $P_{\text{sat}} = 12.5$ mW, $F_{\text{rep}} = 10$ GHz, $L_R = 4$ m, $T_R = 40$ ns, and $\Delta_{AM} = 0.3$. Figure 1 shows the approach to steady state in both the normal- and anomalous-dispersion regimes. It reveals that the pulse converges quickly in the normal-dispersion region but takes > 1000 round trips before converging in the anomalous-dispersion region. Although the rate of convergence depends on the initial conditions used ($E = 1$ fJ, $q = 0$, and $\tau = 0.5$ ps), this type of behavior is expected since the nonlinear effects are weaker in the normal dispersion region. In the normal-dispersion regime the nonlinear effects add to the effect of dispersion and broaden the pulse to $\tau = 3.73$ ps, thus reducing its peak power and the role played by nonlinearity. In the anomalous-dispersion regime the interplay between dispersion and nonlinearity prolongs the convergence. We also point out the robustness of our approach

#6418 - $15.00 US Received 26 January 2005; revised 9 March 2005; accepted 9 March 2005

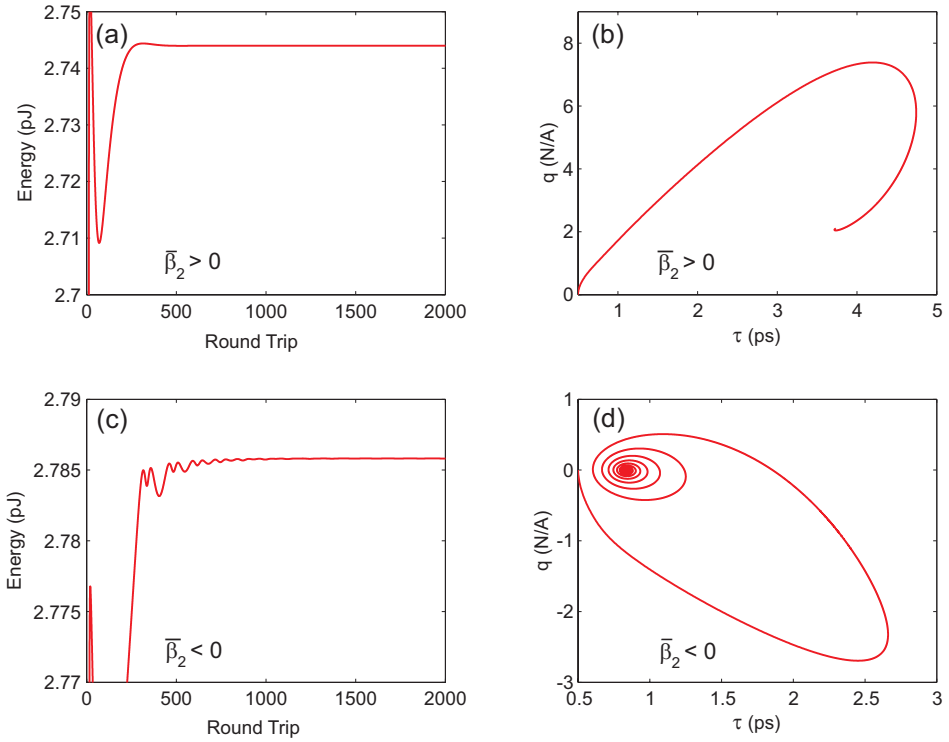

Fig. 1. Changes in pulse energy, width, and chirp over multiple round trips assuming a Gaussian pulse in the normal dispersion regime (top row) and an autosoliton shape in the anomalous-dispersion region (bottom row). The energy scale has been magnified to illustrate that the oscillatory behavior persists for more than 1000 round trips.

since the initial energy used is more than 2500 times smaller than the steady state value obtained.

To quantify the accuracy of our rate-equation model, we solved Eq. (1) numerically with the above parameter values and a 1 photon/mode strength, complex, Gaussian-distributed noise seed. We found that the approach to steady state follows a pattern that is quite close to that seen in Fig. 1. The final steady-state value of pulse width agrees within 2.5% in the case of anomalous dispersion. The agreement is not as good in the case of normal dispersion although it is within 9%. This is a consequence of the pulse shape, which deviates from the Gaussian shape assumed due to nonlinearity, especially for small modulation depths Δ_{AM}.

Figure 1 also reveals the mode-locked pulse in the normal-dispersion regime is chirped ($q \simeq 2$), whereas the chirp is nearly zero ($q \approx 0$) in the anomalous-dispersion regime. This behavior is a consequence of the interplay between dispersion and nonlinearity. In the anomalous regime, the two effects produce chirps with opposite signs, which partially cancel one another, whereas, the chirps add in the normal-dispersion regime [6].

5. Steady-state

As seen in Fig. 1, all pulse parameters converge toward a constant value after a sufficiently large number of round trips. Under steady-state conditions, the derivatives in Eqs. (11)–(13) can be set to zero. This allows us to obtain the following set of coupled algebraic equations for

#6418 - $15.00 US
Received 26 January 2005; revised 9 March 2005; accepted 9 March 2005

the saturated gain, pulse width, and chirp:

$$\bar{g}_{ss} = \left(\bar{\alpha} + \frac{\Delta_{AM}\omega^2\tau_{ss}^2}{2C_5L_R}\right)\left[1 - \frac{T_2^2}{2\tau_{ss}^2}\left(1+q_{ss}^2\right)\right]^{-1}, \tag{14}$$

$$\tau_{ss} = \left(C_4\Delta_{AM}\omega_m^2/L_R\right)^{-1/4}\left[\left(2\bar{\beta}_2/C_1\right)q_{ss} + C_2\bar{g}_{ss}T_2^2\left(C_3 - q_{ss}^2\right)\right]^{1/4}, \tag{15}$$

$$q_{ss} = -d \pm \left[d^2 + C_3 + C_6\bar{\gamma}E\,\tau_{ss}/\left(C_5\bar{\beta}_2\sqrt{2\pi}\right)\right]^{1/2}, \tag{16}$$

where the dimensionless parameter d is defined as

$$d = \frac{1}{2\beta_2}\left[\left(1+C_3\right)\bar{g}_{ss}T_2^2 + \left(\frac{C_1}{C_5} - \frac{C_4}{C_2}\right)\frac{\Delta_{AM}\omega_m^2\tau_{ss}^4}{L_R}\right]. \tag{17}$$

Equation (14) reveals that the saturated gain is determined by the cavity losses, the modulator, and the mode-locked pulse spectrum. Equations (16) and (17) show how the chirp is affected by changing the cavity losses, nonlinearity, or the modulation depth. For example, if the nonlinear parameter is set to zero pulses remain chirped, however, if dispersion is also set to zero, $d \to \infty$ and $q_{ss} = 0$ is the only physically valid solution. Of course, we should use the Gaussian pulse shape under such conditions. Setting $C_n = 1$ in Eq. (15), we find that the steady state pulse width in the absence of dispersive and nonlinear effects is given by

$$\tau_{ss} = \left(\frac{\bar{g}L_R}{\Delta_{AM}}\right)^{1/4}\sqrt{\frac{T_2}{\omega_m}}. \tag{18}$$

This equation is identical to the result first found by Kuizenga and Siegman [1].

The most powerful feature of Eqs. (14)–(16) is that they can be used to instantly (Our theoretical results shown in Fig. 2 took $\ll 1$ second to generate) predict the impact of fiber dispersion and nonlinearity as well as modulation depth and frequency on the mode-locked pulses. Figure 2 shows the results obtained as $\bar{\beta}_2$ and $\bar{\gamma}$ are varied. Plots (a) and (b) investigate the case where dispersion is normal ($\bar{\beta}_2 > 0$); they also reveal a discrepancy between our theory and the full model [i.e. the solution to Eq. (1)]. This error, which is $<$15%, is again due to the pulse shape which deviates from the assumed Gaussian shape. Plots (c) and (d), both made assuming anomalous dispersion, exhibit excellent agreement between our theory and the full model even over the large parameter space explored. Comparing Figs. 2(a) and (c) it is found that as the magnitude of dispersion is decreased, pulse width is reduced but chirp increases. Qualitatively, this behavior is the same in both regions. Comparing Figs. 2(b) and (d), however, we observe an interesting feature. Increasing the nonlinearity in the normal-dispersion region results in a large increase in both pulse width and chirp. However, in the anomalous-dispersion regime, an increase in nonlinearity reduces the pulse width while the chirp increases only slightly. For example, pulse width τ_{ss}, is reduced below 1 ps for $\bar{\gamma} > 0.012$ W^{-1}/m while chirp is nearly zero. If the nonlinearity is increased to $\bar{\gamma} = 0.028$ W^{-1}/m the theory predicts pulses with $\tau_{ss} = 0.36$ ps indicating a pulse 3 times smaller than those predicted by the Kuizenga–Siegman limit [1]. This result was also verified by the full model.

This demonstrates that femtosecond pulses can be realized in actively mode-locked lasers by incorporating elements with large values of $\bar{\gamma}$ into the cavity. Photonic-crystal fibers or tapered fibers can be used for this purpose. Since chirp can be nearly eliminated in the anomalous-dispersion regime, optimized actively mode-locked fiber lasers should produce near transform-limited femtosecond pulses.

6. Conclusion

By applying the moment method to the master equation of mode-locking, we have derived a set of three ordinary differential equations for pulse energy, width, and chirp. These equations play

#6418 - $15.00 US Received 26 January 2005; revised 9 March 2005; accepted 9 March 2005

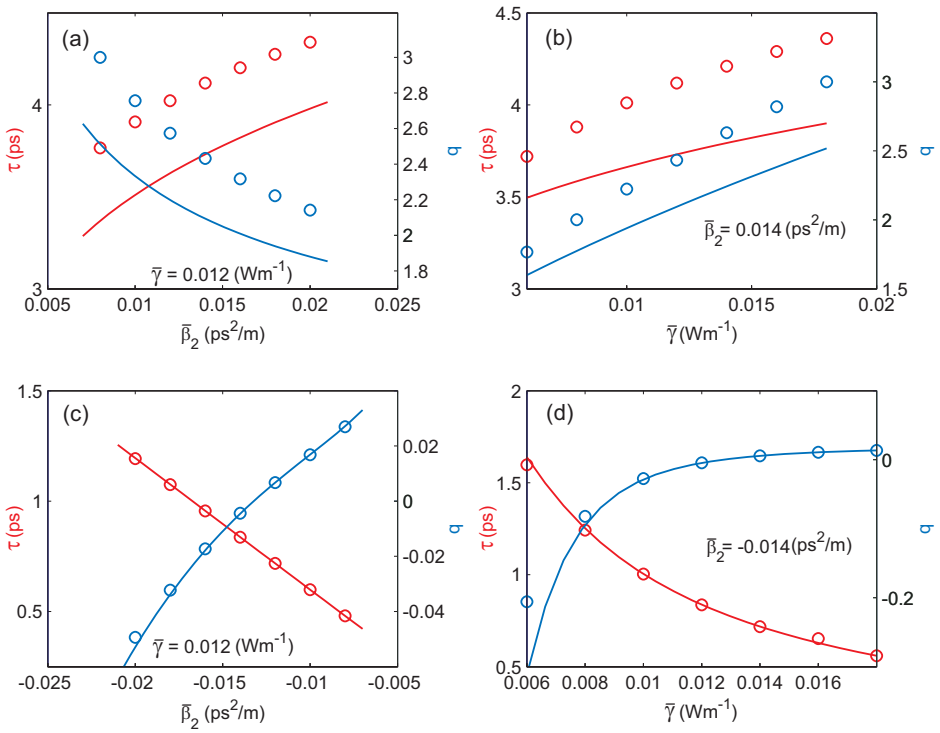

Fig. 2. Steady-state pulse width and chirp as functions of $\bar{\beta}_2$ (left column) and nonlinear parameter $\bar{\gamma}$ (right column). Dispersion is normal for the top row and anomalous for the bottom row. The discrete markers come from solving Eq. (1) while the solid lines come from solving Eqs. (14)–(16).

the role of rate equations for mode-locked lasers. Their solution shows that, although a steady state is eventually reached after sufficiently large number of round trips (in all cases of practical interest), the approach to steady state can be quite different depending on whether the average cavity dispersion is normal or anomalous.

The rate equations reduce to three algebraic equations in the steady state, which were used to study the dependance of pulse width and chirp on cavity dispersion and nonlinearity. We also verified that in the absence of dispersive and nonlinear effects, our analytic result reduces to that obtained in Ref. [1]. Although we have focused on the case of AM mode locking, our approach is quite general and can be applied to all actively and passively mode-locked lasers.

Acknowledgments

This work was supported by the National Science Foundation under grant ECS-0320816 and by the U.S. Department of Energy Office of Inertial Confinement Fusion under Cooperative Agreement No. DE-FC03-92SF19460, the University of Rochester, and the New York State Energy Research and Development Authority. The support of DOE does not constitute an endorsement by DOE of the views expressed in this article.